This is a pre-review manuscript.

The full paper is published in: *Global Change Biology*, 2012; 18:2792–2803

Temperate and tropical brown macroalgae thrive, despite decalcification, along natural CO_2 gradients.

VR Johnson[1,2], BD Russell[3], KE Fabricius[4], C Brownlee[2] & JM Hall-Spencer[1].

[1]Marine Biology and Ecology Research Centre, University of Plymouth, Plymouth, PL4 8AA, UK.

[2] The Marine Biological Association of the United Kingdom (MBA), The Laboratory, Citadel Hill, Plymouth PL1 2PB, UK

[3] Southern Seas Ecology Laboratories, Earth and Environmental Sciences, The University of Adelaide, Adelaide, South Australia, 5005, Australia.

[4] Australian Institute of Marine Science, PMB 3, Townsville, Queensland 4810, Australia.

Corresponding Author: Jason Hall-Spencer

Email: jhall-spencer@plymouth.ac.uk

Keywords: ocean acidification, calcification, photosynthesis, temperate and tropical coastal ecosystems.

Abstract

Predicting the impacts of ocean acidification on coastal ecosystems requires an understanding of the effects on macroalgae and their grazers, as these underpin the ecology of rocky shores. A range of studies show that calcified coralline algae (Rhodophyta) may be especially vulnerable to ocean acidification, but there is a lack of information concerning calcified brown algae (Phaeophyta). Here we compare ecological shifts in sub-tidal rocky shore systems along CO_2 gradients created by volcanic seeps in the Mediterranean and off Papua New Guinea. In both the temperate and tropical systems the abundance of grazing sea urchins fell dramatically along CO_2 gradients. Temperate and tropical species of the calcifying macroalgal genus *Padina* (Dictyoaceae, Phaeophyta) showed reductions in $CaCO_3$ content with CO_2 enrichment. In contrast to other studies of calcified macroalgae, however, we observed an increase in the abundance of *Padina* spp in acidified conditions. Reduced sea urchin grazing pressure and significant increases in photosynthetic rates may explain the unexpected success of decalcified *Padina* spp. at elevated levels of CO_2. Replicated observations are required across regions to increase confidence in predictions of the ecological impacts of ocean acidification on a global scale.

Introduction

Rising anthropogenic emissions of CO_2 are rapidly altering ocean chemistry since increasing pCO_2 in seawater has already lowered the mean ocean surface pH by 0.1 units from pre-

50 industrial values, with a predicted further decrease of 0.3-0.4 units by 2100 (IPCC, 2007).
51 The resulting decrease in calcium carbonate saturation levels compromises the ability of
52 many marine organisms to form shells and skeletons (Orr *et al*., 2005; Doney *et al*., 2009).
53 This, in combination with the diverse responses of photosynthetic organisms to increased
54 pCO_2 levels (Russell *et al*., 2009; Hepburn *et al*., 2011; Johnson *et al*., 2011; Porzio *et al*.,
55 2011), is expected to alter the structure of biological communities along coastlines worldwide
56 (Barry *et al*., 2011). However, the potential effects of altered community structure on
57 ecosystem functioning are unclear since the effects of elevated CO_2 levels on organism
58 interactions have only recently begun to be addressed (Diaz-Pulido *et al*., 2011; Doropoulous
59 *et al*., 2012).
60
61 Seagrasses and many macroalgal species are notably tolerant of increases in CO_2 (Connell &
62 Russell, 2010; Fabricius *et al*., 2011; Porzio *et al*., 2011; Roleda *et al*., 2011). However,
63 studies from polar, temperate and tropical latitudes have revealed that settlement,
64 calcification, growth and abundance of calcified macroalgae can be negatively affected by
65 increasing CO_2 levels since this lowers carbonate saturation states which can corrode the
66 algal skeletons (Kuffner *et al*., 2008; Martin *et al*., 2008; Martin & Gattuso, 2009; Robbins *et*
67 *al*., 2009; Russell *et al*., 2009; Büdenbender *et al*., 2011; Price *et al*., 2011; Sinutok *et al*.,
68 2011; Doropoulos *et al*., 2012). Increasing concentrations of CO_2 can, on the other hand,
69 enhance productivity and growth in both non-calcified (Gao *et al*., 1993a; Kübler *et al*., 1999;
70 Connell & Russell, 2010) and calcified macroalgae (Reiskind *et al*., 1988; Gao *et al*., 1993b;
71 Semesi *et al*., 2009).
72
73 Understanding the effects of ocean acidification on calcified algae is a high priority as they
74 play a crucial role in the ecology of coastal ecosystems (Nelson, 2009). Most studies to date

have been single species laboratory experiments that last a year at most (Martin & Gattuso, 2009). Such experiments provide important information on species' responses to increased pCO_2 but fail to account for the effects of long-term exposure. They are also unrepresentative of natural ecosystems since, for example, they remove the effects of species interactions (Barry *et al*., 2011). Consequently, there is a great need for studies targeting interactions between multiple species in order to assess the effects on strength of competition, predation and/or herbivory (Wernberg *et al*., in press). Here we assess the abundance of herbivores (sea urchins) and the response of brown macroalgae (*Padina* spp.) to increasing levels of CO_2 in natural settings, as interactions between these groups of organisms can drive ecological changes in benthic habitats on temperate (Sala, 1998; Hernández *et al*., 2008) and tropical shores (McClanahan, 1994; Mumby *et al*., 2006).

Padina is one of only two genera of Phaeophyta that calcify and is an important producer of calcium carbonate and organic matter in both temperate and tropical shallow waters (Bathurst, 1971; Milliman, 1974). Calcium carbonate is deposited as aragonite needles on the surface of fan-shaped thalli, forming concentric bands of white precipitate (Okazaki *et al*., 1986). Carbonate production rates of *Padina* sp. in one sub-tropical system have been calculated to be around 240 $gm^{-2}\ yr^{-1}$, considerably higher than for other erect calcified algal genera such as *Halimeda* (50 $gm^{-2}\ yr^{-1}$) and *Penicillus* (30 $gm^{-2}\ yr^{1}$) (Wefer, 1980). Several roles have been suggested for calcification in macroalgae. It is thought to offer structural defence, providing mechanical resistance to herbivores and minimising grazing damage to tissues (Littler & Littler, 1980; Padilla, 1993), increase the ability of bicarbonate and nutrient assimilation through the generation of protons (McConnaughey & Whelan, 1997), improve photosynthetic performance (McConnaughey, 1998) and provide protection from excess irradiance (Bürger & Schagerl, 2010). Therefore changes in macroalgal calcification as a

result of ocean acidification have the potential to alter physiological and ecological fitness, by altering photosynthetic efficiency, thallus rigidity, growth rates and mortality (Nelson, 2009).

Ocean acidification also has the potential to reduce top-down biological control of benthic biodiversity (Widdicombe and Spicer, 2008). Sea urchins are dominant grazers in many marine habitats and play an important role in controlling the structure and composition of macroalgal communities. They often act as keystone species (Sala *et al*., 1998) and, as a consequence, reduction in their abundance or removal from an ecosystem can result in rapid colonisation of benthic habitats by macroalgae (Villouta *et al*., 2001; Behrens & Lafferty, 2004). Sea urchins are particularly susceptible to reductions in pH (Miles *et al*., 2007) and a mean pH of 7.8 appears to be the critical level below which Mediterranean sea urchins do not survive (Hall-Spencer *et al*., 2008). Adverse impacts of ocean acidification on echinoderms would be likely to have significant consequences at the ecosystem level (Barry *et al*., 2010; Dupont *et al*., 2010). It has the potential to release algae from the control of grazing by sea urchins, resulting in cascade effects throughout benthic food webs, with potentially profound implications for the structure and function of marine communities.

Natural CO_2 gradients are beginning to reveal the ecological shifts that can be expected to occur with globally increasing atmospheric CO_2 in both temperate (Hall-Spencer *et al*., 2008) and tropical ecosystems (Fabricius *et al*., 2011). Work has begun to understand the underlying mechanisms that cause ecological shifts along these CO_2 gradients, such as the influence of recruitment success (Cigliano *et al*., 2010) and the combined physiological effects of temperature and CO_2 (Rodolfo-Metalpa *et al*., 2011). The aim of this study was to survey populations of *Padina* spp. (Dictyotaceae) and sea urchins (Echinoidea) along pH gradients in both temperate and tropical ecosystems and to measure *in situ* effects of elevated

CO_2 on calcification and photosynthesis in this common phaeophyte. We present data on the long- term effects of natural exposure to low pH and high CO_2 on *Padina pavonica* (Linnaeus) Thivy at shallow CO_2 seeps on the island of Vulcano, NE Sicily and on *Padina australis* Hauck at comparable seeps in the D'Entrecasteaux Island group, Papua New Guinea. To our knowledge, this is the first study to compare ecological responses to CO_2 gradients in temperate and tropical systems. We observed strikingly similar ecological shifts along both tropical and temperate rocky shores as CO_2 levels increased to those previously recorded at CO_2 vents off Ischia, Italy (Hall-Spencer *et al*., 2008), with the loss of sea urchins and coralline algae together with an increased abundance of pheaophytes.

Material and Methods

Temperate and tropical rocky shore surveys

149 *Padina pavonica* was sampled along a stretch of rocky coast off the island of Vulcano
150 (38°25' N, 14°57' E, part of the Aeolian Island chain, NE Sicily) in September 2010 and May
151 2011 (see maps in Johnson *et al*., 2011). This is a microtidal region where volcanic CO_2 vent
152 activity acidifies the seawater producing a pH gradient ranging from ~ 8.2 to ~6.8, running
153 parallel to the coast. Within the vent area, three shallow (< 0.5 m depth) sampling stations
154 were selected as they lay along a CO_2 gradient, characterised by intermediate to low mean pH
155 (V-S1 pH 8.06, CI = 0.59%; V-S2 pH 7.54, CI = 1.59%; V-S3 pH 7.46, CI = 2.03%, *n* = 24-
156 27). Three reference stations located outside the vent area were selected on the basis of their
157 normal, relatively stable pH (V-R1 pH 8.17, CI = 0.42%; V-R2 pH 8.18, CI = 0.32%; V-R3
158 pH 8.19, CI = 0.28%, *n* = 22-24). Four additional sampling stations were selected along the
159 gradient, one located between S2 and S3 (at mean pH 7.97, CI = 1.45%, *n* = 16) and three at
160 20 m intervals between S1 and the end of the gradient (at mean pH 8.08, CI = 0.82%; pH
161 8.16, CI = 0.33%; pH 8.20, CI = 0.23%, *n* = 6-22) to allow *P. pavonica* and sea urchin
162 abundance surveys to occur along the full length of the CO_2 gradient. Temperature, total
163 alkalinity, salinity and light levels were relatively constant in the shallow sub-tidal region
164 along this gradient (Johnson *et al*., 2011).
165
166 *Padina australis* was sampled along the shallow (0.1-0.3 m, below lowest astronomic tide)
167 shore of two sites in Milne Bay Province, Papua New Guinea (9°45' S, 150°50' E): Upa-
168 Upasina and Esa'Ala along the north-western and north-eastern coast off Normanby Island
169 (see maps in Fabricius *et al*., 2011) in April 2011. Tidal range in the region is <1 m. Volcanic
170 CO_2 seeps acidify the seawater, with seeping being most intense near the shore at <0.5 m
171 depth. In these shallow shore zones, reductions in pH were greater than recorded for coral
172 reef habitats by Fabricius *et al*., (2011). Two sampling stations of intermediate to low mean
173 pH were selected at both Upa-Upasina (U-S1 pH 7.78, CI = 0.26%; U-S2 pH 7.49, CI =

0.62%, *n* = 7) and Esa'Ala (E-S1 pH 7.86, CI = 1.30%; E-S2 pH 6.68, CI = 4.53%, *n* = 7-9). Reference stations with normal, relatively stable pH (U-R1 pH 8.31, CI = 0.12%; U-R2 pH 8.22, CI = 0.10%; E-R1 pH 8.19, CI = 0.77%, *n* = 6-9) were chosen several hundred meters away from the seeps at comparable geophysical settings.

At all sites (Vulcano in the Mediterranean, and Upa-Upasina and Esa'Ala in Papua New Guinea), 20 quadrats (50 cm x 50 cm) were placed haphazardly within 15 x 3 m survey zones (<0.5 m depth) at each station along the CO_2 gradients. Within each quadrat the percentage cover of *Padina* spp. was estimated and the total number of sea urchins (*Paracentrotus lividus* & *Arbacia lixula* in the Mediterranean, *Diadema* spp. & *Echinometra* sp. in Papua New Guinea) recorded.

Carbonate chemistry measurements

A calibrated pH meter was used to measure pH (NBS scale) at each sampling station at Vulcano (YSI 556 MPS, three-point calibration) and Papua New Guinea (Hach or Oakton, two-point calibration, with readings cross-checked against a Tris buffer seawater standard). Temperature and salinity were also measured alongside each pH reading. We recorded rapid pH fluctuations along this coastal gradient (over 1 unit in under ~ 4 hours at S3 at Vulcano), so the uncertainty inherent in using the NBS scale for seawater measurements (approximately 0.05 pH, Dickson *et al*., 2010) was considered acceptable for this study. Mean pH (back-transformed hydrogen ion concentrations) were calculated for each station at Vulcano (pH sampled on several occasions; September-October 2009, April 2010, July 2010, September-October 2010, May 2011, September-October 2011, *n* = 22-27) and Papua New Guinea (25th

199 and 29th April 2011, *n* = 6-9). 95% confidence intervals were calculated and presented as a
200 percentage of the mean pH.
201
202 Total alkalinity (TA) was measured alongside pH to calculate the other parameters
203 constraining the carbonate chemistry of the seawater (Hoope *et al*., 2010). At Vulcano, TA
204 was measured at each station, on three separate visits (Sept 2010, May 2011 and Sept 2011),
205 from a water sample after 0.2 µm filtration and storage in the dark at 4°C, using an AS-Alk 2
206 Total Alkalinity Titrator (Apollo SciTech Inc, Georgia, USA). Total alkalinity data for Papua
207 New Guinea were taken from Fabricius *et al*., (2011). The remaining parameters of the
208 carbonate system were calculated using the CO2 SYS software (Lewis & Wallace, 1998).
209
210 *Padina spp. calcium carbonate analysis*
211
212 Large (>2 cm) *Padina* spp. fronds were collected from each sampling station at Vulcano in
213 the Mediterranean (*n* = 30 per station) and from a reference and high CO_2 station at both
214 Upa-Upasina (U-R1 & U-S1, *n* = 15 per station) and Esa'Ala (E-R1 & E-S2 *n* = 5 per station)
215 in Papua New Guinea. Samples were stored in 70% ethanol until analysis. Calcium carbonate
216 ($CaCO_3$) content of each frond was determined through a weight loss after acidification
217 protocol (Martone, 2010). Fronds were dried, weighed, decalcified in hydrochloric acid (1N)
218 and then re-dried and reweighed. The $CaCO_3$ content, expressed as a percentage of dry
219 weight, was calculated from the difference between dried mass and decalcified dry mass.
220
221 Images of *P. pavonica* aragonite crystals were examined for size and abundance with
222 scanning electron microscopy (JEOL JSM 5600 LV). Three fronds from each station were
223 fixed in glutaraldehyde for 1-2 hours, and then stored in 1x PBS buffer (phosphate buffered

saline) until examination. As the size and number of crystals has been reported to vary with age of frond segment (Hills-Colinvaux, 1980), we only compared the apical segments of *P. pavonica* fronds between stations. Prior to viewing under the SEM, samples were air dried, mounted on aluminium stubs with carbon adhesive tape and coated in gold. For each of the 18 samples, 5 images were taken at random locations (using image coordinates and random number generator) over calcified regions of the apical surface only (see images in Fig. 5) and the average length and width of 10 randomly selected crystals per image was measured digitally using Image J software (v 1.43, National Institutes of Health, Bethesda, MD, USA). In addition, for each image, the number of crystals within a randomly selected 5µm x 5µm area were counted and averaged for each frond.

Photosynthesis in P. pavonica

Photosynthetic condition and performance of *P. pavonica* at Vulcano was investigated through measurements of photosynthetic pigment (Chl *a* and c_1+c_2) concentrations and Chl *a* fluorescence. Fronds were collected from each sampling site at Vulcano in September 2010 and September 2011 (n = 40 per station), rinsed in distilled water and frozen for transportation back to the laboratory. Fronds were collected between 8am-10am to avoid the confounding effect of light intensity, in particularly mid-day photoinhibition, on chlorophyll content (Hädar *et al*., 1996). To prevent chlorophyll degradation during storage, samples were kept at -20 °C in the dark during the sampling period on Vulcano and at -80 °C when longer periods occurred before analysis. Chlorophyll was extracted from all samples within < 2 weeks of sampling.

Prior to extraction, fronds (~ 0.70 g samples) were homogenized in 90% acetone by pestle and mortar. Chlorophyll was extracted in 90% acetone at 4°C for 24 hours in the dark. The absorbance of each sample at 630, 664 and 750 nm (background absorbance) was measured (3 replicate readings were taken from each sample to obtain an average) using a Cecil CE2011 spectrophotometer. The concentration of chlorophyll *a* and *c* ($c_1 + c_2$) in the sample was calculated using the equations of Ritchie (2006). The volume of the solvent (in weight / g) and the weight of the frond were then used to provide a final calculated reading of chlorophyll (μg mg^{-2} fresh weight). Values for both September sampling periods were pooled to calculate a mean for each station.

In May 2011 the effective quantum yield (Y) and relative electron transport rates (*r*ETR) of freshly collected, light-adapted fronds (n = 6 per station), were measured in small dishes using a Diving PAM fluorometer (Walz-Germany).

$$Y = F'_m - F_t / F'_m \text{ (Genty, 1989)}$$

$$r\text{ETR} = \text{Y x PAR x 0.5 (Beer } et\ al.\text{, 1998)}$$

Rapid light curves (RLC) were applied to assess the light saturation behaviour of fronds across each of the six sampling stations in Vulcano. RLC data can be useful for assessing photosynthetic capacity and potential over a wide range of ambient light intensities (Ralph & Gademann, 2005). The Diving-Pam was set to deliver red pulse-modulated light at 655 nm followed by steps of actinic light every 20 s (other settings: gain = 4, actinic light factor = 0.5, light curve intensity y = 5, saturation width = 0.8, saturation intensity = 3, signal damping = 2).

Statistical analyses

To test for significant effects of mean pH on variations in *Padina* spp. we used generalised linear models (GLM), with pH as the explanatory variable and Site (Vulcano, Upa Upasina and Esa'Ala) as a covariate. Data were averaged across stations and transformed where necessary to approximate normality and equal variance. For count data with many zeroes (e.g., sea urchin abundances) or over-dispersed data, a quasi-poisson link function was used, whereas for proportional, ETR and yield data, a quasi-binomial link function, and for the remaining data the Gaussian link function were used. All statistical analyses were performed using R (R Development Core Team, 2012).

Results

Seawater chemistry

Table 1 shows the range in carbonate chemistry parameters for each sampling station. The median pCO_2 levels (calculated from median pH and mean TA) were lowest in the reference stations (276-388 µatm) and increased with proximity to the CO_2 seeps, with the highest values recorded at V-S3 (1428 µatm), U-S2 (2665 µatm) and E-S2 (23,095 µatm). The mean pH of the reference stations ranged from 8.17 to 8.31, while the mean pH at the seep stations ranged from 8.06 to 6.68, with increasing variance towards lower values (Fig. 1). The highest median values for pCO_2 and DIC were found at V-S3 (1428 µatm and 3.79 mmol kg^{-1} respectively), U-S2 (2665 µatm and 2.03 mmol kg^{-1}) and E-S2 (23,095 µatm and 2.85 mmol kg^{-1}). Calcium carbonate was under-saturated at E-S2 and periods of under saturation occurred during the lowest range of pH at V-S3 (Ω 0.15 calcite and Ω 0.09 aragonite) and U-S2 (Ω 0.98 aragonite).

Padina spp. and sea urchin abundances

There were dramatic ecological shifts along all three volcanic seeps as CO_2 levels increased. We observed a loss of sea urchins and coralline algae together with an increased abundance of phaeophytes that was strikingly similar to that recorded at CO_2 vents in Ischia, Italy (Fig 2a & b). These shifts were detected at median pCO_2 levels of 510 µatm (median pH 8.08), 1218 µatm (median pH 7.78) and 914 µatm (median pH 7.89) along the gradients at Vulcano, Upa Upasina and Esa'Ala, respectively (Fig. 3). Benthic cover of *Padina* spp. increased with rising CO_2 and was two-three fold greater in the highest CO_2 stations (V-S3, U-S2 & E-S2) relative to the reference stations (Fig. 3). We detected a significant effect of pH on *Padina* spp. benthic cover and sea urchin abundance at all three gradients (GLM: Table 2). In contrast to *Padina* spp., sea urchin abundance was greatest at the reference stations and

323 decreased with declining pH at all three gradients (Fig. 3 a-c, Table 2). Sea urchins were
324 absent at stations with the highest levels of pCO_2 (V-S1-S3, U-S2, E-S2).
325
326 *Physiological responses of Padina spp. to elevated CO_2*
327
328 We found that pH had a statistically significant effect on the $CaCO_3$ content in *Padina* spp.
329 fronds at Vulcano only (as smaller sample sizes were taken at Upa-Upasina and Esa'Ala;
330 Fig.4, Table 2). At Vulcano, $CaCO_3$ content in *P. pavonica* was highest at the reference
331 stations (57-63%) and decreased significantly in the CO_2 enriched stations; S1 (35% ± 1.4),
332 S2 (15% ± 1.3) and S3 (14% ± 0.9). Analysis of *P. australis* from Upa-Upasina in Papua
333 New Guinea also revealed a large reduction in $CaCO_3$ content from 55 % ± 1.7 at the
334 reference station (U-R1) to 35% ± 3.6 at the intermediate station (U-S1). At Esa'Ala, $CaCO_3$
335 content was considerably greater in fronds from the reference station (E-R1: 66% ± 7.1)
336 compared with those the highest CO_2 exposure station (E-S2: 40% ± 1.8).
337
338 Table 3 shows the abundance and morphometric data of the aragonite crystals on the surface
339 of *P. pavonica* fronds. Over the thin calcified bands in the apical regions we detected a
340 significant increase in crystal abundances with declining pH (GLM: slope of square root
341 transformed data = -0.23 ± 0.077, t = -2.99, $P = 0.037$) and a reduction in the width of
342 crystals (slope = 0.23 ± 0.067, t = 3.42, $P = 0.026$), but no effect on crystal length ($P = 0.85$).
343
344 The pH had a significant effect on the content of both chlorophyll *a* and chlorophyll *c* in *P.*
345 *pavonica* (Fig. 5, GLM: slope = -0.24 ± 0.065, t = -3.78, $P = 0.019$; slope = -0.028 ± 0.0055, t
346 = -5.21, $P = 0.006$, for chlorophyll *a* and *c*, respectively). Both the chlorophyll a and c
347 content increased with declining pH (Chl *c*: V-S1= 0.05 mg g^{-1}fw ± 0.002, V-S2 = 0.06 mg g^{-}

348 ^{1} fw ± 0.002, V-S3= 0.07 mg g^{-} fw ± 0.003 compared with those in the reference stations: V-
349 R1= 0.04 mg g^{-1} fw ± 0.002, V-R2= 0.04 mg g^{-1} fw ± 0.004, V-R3= 0.04 mg g^{-1} fw ± 0.003).
350
351 The differences observed in the photosynthetic responses of *P. pavonica* to increased CO_2 are
352 presented in a rapid light curve in Fig. 6. The *r*ETR max values significantly increased with
353 declining pH (GLM: slope on forth-root transformed data = -0.54 ± 0.091, t = -5.97, *P* =
354 0.004). We also detected a significant effect of pH on the *r*ETRs recorded at supersaturating
355 irradiance; 3344 μmol quanta m^{-2} s^{-1} (slope on forth-root transformed data = -0.49 ± 0.098, t
356 = -4.95, *P* = 0.008) where the greatest values were recorded at S2 and S3 (137.43 μmol
357 electrons m^{-2} s^{-1} ± 10.12, 134.45 ± 7.97 respectively), however no significant effect of pH
358 on the *r*ETRs under a subsaturating irradiance (360 μmol quanta m^{-2} s^{-1}) could be detected
359 (slope on forth-root transformed data = -0.12 ± 0.049, t = -2.55, *P* = 0.063). We also failed to
360 detect a significant effect of pH on the photochemical efficiencies (*F*v/*F*m) of *P. pavonica* (*P*
361 = 0.35).
362
363
364 **Discussion**
365
366 To our knowledge, this is the first *in situ* demonstration of the effects of elevated CO_2 on
367 grazer-algal population dynamics. It is also the first to provide a comparison of ecological
368 changes along CO_2 gradients between temperate and tropical rocky shores. Along both
369 temperate and tropical rocky shores there was a reduction in sea urchin abundances alongside
370 a proliferation of *Padina* spp., as CO_2 levels increased. We propose that the elevated CO_2
371 levels may influence algal-grazer dynamics as species assemblages change, causing profound
372 structural and functional changes in rocky shore habitats. The changes in benthic community

composition were detected at threshold pCO_2 levels of ~500 µatm in Sicily and therefore, according to climate change predictions (IPCC, 2007), indicate that we may begin to witness these ecological shifts occurring in temperate rocky shores from around the midpoint of this century. Threshold values of pCO_2 for the rocky shore shifts in Papua New Guinea were considerably higher (> 900 µatm) than those in Sicily, this may be due to the relatively limited range of CO_2 enriched sampling stations in Papua New Guinea. Investigating the benthos at more intermediate levels of CO_2 may have revealed lower threshold values for ecological shifts, similar to those in Sicily.

Our present knowledge of the effects of ocean acidification on calcified macroalgae is mostly derived from studies investigating the impacts of high CO_2 on calcifiers with high magnesium calcite skeletons, such as the family Corallinaceae (Anthony *et al*., 2008; Kuffner *et al*., 2008; Martin *et al*., 2008; Martin & Gattuso, 2009; Semesi *et al*., 2009; Gao & Zheng, 2010; Büdenbender *et al*., 2011) and as a consequence, aragonitic algae have been relatively overlooked. Furthermore, the responses of calcified Pheaophyta are virtually unknown (Porzio *et al*., 2011). To our knowledge, this is the first study to investigate the *in situ* impacts of elevated CO_2 on calcification and photosynthesis in *Padina* spp.

Unexpected responses of Padina spp. to elevated CO_2

Our present knowledge concerning the impacts of ocean acidification has raised concern for the future success of calcified macroalgae under conditions of high CO_2. Previous investigations at CO_2 vent seeps have observed dramatic reductions in the abundance of calcified macroalgae (Hall-Spencer *et al*., 2008; Martin *et al*., 2008; Fabricius *et al*., 2011). The results from this investigation, however, indicate that some calcified algae may thrive as

398 the oceans acidify despite expected reductions in calcification. We discovered that tropical
399 and temperate *Padina* spp. can proliferate with CO_2 enrichment, as similarly recorded for
400 some genera of fleshy macroalgae (Hall-Spencer *et al*., 2008; Fabricius *et al*., 2011; Porzio *et*
401 *al*., 2011).
402
403 In both *P. pavonica* and *P. australis*, the content of $CaCO_3$ in thalli decreased with reductions
404 in pH. This is consistent with other calcification studies on aragonitic macroalgae (Price *et*
405 *al*., 2011; Sinutok *et al*., 2011) and high magnesium calcitic macro algae (Martin & Gattuso,
406 2009; Semesi *et al*., 2009). Reductions in $CaCO_3$ content implies that *Padina* spp. herbivore
407 defence may be compromised under low pH, potentially leading to an increase in grazing
408 mortality and reduction in benthic cover. This was not, however, reflected *in situ*. Sea urchins
409 are major grazers on *Padina* spp. and their presence can cause significant reductions in the
410 abundance of these algae in the Mediterranean (Hereu *et al*., 2006) and in the tropics
411 (Sammarco, 1982). Our recorded absence of sea urchins in the CO_2 enriched areas may
412 therefore explain the proliferation of *Padina* spp., as it becomes released from the top-down
413 control of these keystone grazers. Similar effects of sea urchin removal have been observed
414 in other *Padina* sp. populations (Sammarco *et al*., 1974) and across other Phaeophyte
415 assemblages (Leinaas & Christie, 1996; Ling *et al*., 2010).
416
417 *Photosynthetic response of Padina pavonica to elevated CO_2*
418
419 Increased productivity with elevated CO_2 may contribute to the success of *Padina* at low pH.
420 Laboratory studies of other calcified macroalgae have revealed declines in photosynthetic
421 pigments in high CO_2 / low pH treatments (Gao and Zheng, 2010; Sinutok *et al*., 2011) which
422 are indicative of chlorophyll degradation, a reduction in photosynthetic unit size and/or a

423 reduction in PSII reaction centres (Sinutok *et al*., 2011). Our findings, however, show the
424 opposite. We found that Chl *a* and Chl *c* content in *P. pavonica* was greater in the CO_2
425 enriched stations indicating an increase in photosynthetic capacity under conditions with high
426 CO_2. It has been speculated that pH stress may negatively impact photosynthetic performance
427 through the disruption of the CO_2 accumulating pathway at the site of Rubisco, or
428 interference with electron transport (Anthony *et al*., 2008). This has been supported though
429 laboratory experiments with *Halimeda* spp. which have demonstrated declines in
430 photosynthetic efficiency (Sinutok *et al*., 2011) and response (Price *et al*., 2011) under
431 elevated CO_2. In contrast, we did not observe significant effect of pH on photosynthetic
432 efficiency (Fv/Fm), along gradients of CO_2. Indeed, we found a significant effect on the *in*
433 *situ* photosynthetic responses of *P. pavonica* with CO_2 enrichment (increases in $rETR_{max}$ and
434 mean $rETR_{max}$ at supersaturating irradiance). *Padina pavonica* is not carbon-saturated in
435 seawater and can utilise more inorganic carbon if it is provided as CO_2 (Einav *et al*., 1995).
436 The positive photosynthetic response of *P. pavonica* to CO_2 enrichment therefore indicates a
437 direct enhancement of carbon fixation across the gradient. Increased photosynthetic activity
438 at high CO_2 has also been observed in other calcified macroalgae (Reiskind *et al*., 1988, Gao
439 *et al*., 1993b, Semesi *et al*., 2009) and non-calcified macroalgae (Gao *et al*., 1993a; Kübler *et*
440 *al*., 1999; Connell & Russell, 2010; Russell *et al*., 2011b).
441
442 It has been established that photosynthesis can stimulate calcification in algae (Borowitzka,
443 1982; Gattuso *et al*., 1999). The co-existence of chloroplasts and aragonite deposition in the
444 same thallus region of *Padina* indicates an intimate relationship between calcification and
445 photosynthesis (Okazaki *et al*., 1986). Increased $CaCO_3^-$ dissolution in lower pH may
446 therefore be offset by increased photosynthesis in those regions with chloroplasts. This may
447 help to explain why we found that even in the lowest pH conditions, *P. pavonica* and *P.*

australis were still able to calcify, seemingly from the enhancement of photosynthesis under high levels of CO_2. Alternatively, the high pH variability in the vent zone, caused by transient exposure to ambient pH conditions (i.e periods of high winds increasing the mixing of vent waters with surrounding high pH seawater), has the potential to buffer the effects of acidification by relieving physiological stress (Hoffmann *et al*., 2011).

Implications of elevated CO_2 on Padina spp. calcification

There is a lack of laboratory evidence of the effects of low pH on *Padina* spp. calcification to confirm whether decreased calcification is a direct response to reduced pH as opposed to, for example, the reduced grazing pressure in this *in situ* experiment. An investigation of Caribbean *Padina* sp. (Lewis *et al*., 1987) however, revealed that in heavily grazed areas the algae existed in the form of an uncalcified turf whereas in areas of low grazing activity it grew as calcified, foliose blades. The fact that these algae still calcify when grazing intensity is low suggests that the reduced calcification recorded in this study may indeed be a direct response to lowered pH and not the changes in grazing pressure. It has been suggested that calcium carbonate crystal morphology and abundance may be associated with seawater chemistry: thinner, more abundant crystals have been shown to indicate reduced pH conditions as crystallisation events are thought to be initiated and terminated more frequently (Robbins *et al*., 2009; Sinutok *et al*., 2011). Over the thin calcified band in the apical region of *P. pavonica* fronds in the CO_2 enriched stations, we recorded more abundant aragonite crystals than in the reference stations and we also observed a decreasing trend of crystal width with increasing levels of CO_2. These results therefore support the theory of pH dependent changes in calcium carbonate crystal morphology and deposition in calcified

472 macroalgae. The implications of changes in *Padina* spp. bio-calcification on thallus rigidity,
473 dissolution rates and overall sediment budgets however, need further investigation.
474
475 **Conclusions**
476
477 Volcanic CO_2 vent systems are revealing the changes in ecological interactions and
478 community shifts we can expect in subtidal rocky shore ecosystems under elevated CO_2. This
479 study reveals dramatic shifts in benthic community structure that were strikingly similar to
480 those documented at anther CO_2 vent site in Italy (Hall-Spencer *et al*., 2008). Our study
481 shows that certain calcified phaeophytes could, in fact, be amongst the ecological winners
482 under ocean acidification scenarios, alongside fleshy macroalgae (Kübler *et al*., 1999; Porzio
483 *et al*., 2011; Raven *et al*., 2011). This may be explained by a combination of; reduced sea
484 urchin predation (and presumably other calcareous predators such as gastropods), increased
485 photosynthetic capacity and performance and optimised energy reallocation following a
486 reduction in carbon limitation. This work adds to evidence for proliferation of phaeophytes in
487 a high CO_2 world (Hall-Spencer *et al*., 2008; Connell & Russell 2010; Diaz-Pulido *et al*.,
488 2011; Russell *et al*., 2011b) and has potentially profound consequences for the structure,
489 function and resilience of a variety of benthic ecosystems globally (Russell *et al*., 2009;
490 McManus & Polsenberg, 2004; Harries *et al*., 2007).
491
492 Large differences in the impacts of CO_2 enrichment between *Padina* spp. and other calcified
493 species have been made apparent by this study. This highlights the importance of studying a
494 wide range of genera to better inform global predictions of the impacts of ocean acidification
495 on marine ecosystems (Russell *et al*., 2011a). This study has demonstrated that the response
496 of *Padina* spp. to CO_2 enrichment is complex and potentially multi-factorial. An *in situ*,

ecosystem based approach, incorporating multi-species interactions and predator-prey dynamics, provides more accurate insights into the responses of marine organisms, highlighting the importance of natural CO_2 gradients as a valuable tool in the study of ocean acidification. The similarities we found in the responses of *Padina* spp. and sea urchin abundance at several vent systems increases the robustness of our predictions over a large geographical range. Similar comparisons should be adopted for other marine biota in future ocean acidification studies.

Acknowledgements

VJ thanks the Marine Institute, University of Plymouth (UoP) for PhD funding and the staff at the Marine Biological Association UK and the SEM unit at UoP for laboratory support. M Milazzo and M Graziano at the University of Palermo provided field assistance and pH data in Sicily, and A Beesley at Plymouth Marine Laboratory performed total alkalinity analyses. Special thanks to the Traditional Owners of the Illi Illi Bwa Bwa and Esa'Ala reefs for allowing us to survey their reefs. This work contributes to the EU FP7 project 'Mediterranean Sea Acidification under a changing climate' (grant agreement no. 265103), with additional funding for JHS from Save Our Seas Foundation. Funding for the PNG study was provided by the Australian Institute of Marine Science and an International Science Linkages Grant of the Australian Commonwealth Department of Innovation, Industry, Science and Research. An Australian Research Council grant funded BDR.

References

Anthony KRN, Kline DI, Diaz-Pulido G, Dove S, Hoegh-Guldberg O (2008) Ocean acidification causes bleaching and productivity loss in coral reef builders. *Proceedings of the National Academy of Sciences*, **105**, 17442–17446.

Barry JP, Widdicombe S, Hall-Spencer, JM (2011). Effects of ocean acidification on marine biodiversity and ecosystem function. In Gattuso, J-L and Hansson, L. (eds) Ocean Acidification, Oxford University Press, Chapter 10: 192 -209

Bathurst RGC (1971) Carbonate sediments and their diagenesis. pp 1-620. Elsvier, Amsterdam.

Beer S, Vilenkin B, Weil A, Veste M, Susel L, Eshel A (1998) Measuring photosynthetic rates in seagrasses by pulse amplitude modulated (PAM) fluorometry. *Marine Ecology Progress Series*, **174**, 293–300.

Behrens MD, Lafferty KD (2004) Effects of marine reserves and urchin disease on southern Californian rocky reef communities. *Marine Ecology Progress Series*, **279**, 129-139.

Borowitzka MA (1982) Mechanisms in algal calcification. *Progress in Phycological Research,* **1**, 137-177.

Bürger K, Schagerl M (2010) Morphological studies of the brown alga *Padina pavonica* (L.) Thivy. Unpublished Master Thesis, Department of Marine Biology, University of Vienna, Vienna.

Büdenbender J, Riebesell U, Form A (2011) Calcification of the Artic coralline red algae *Lithothamnion glaciale* in response to elevated CO_2. *Marine Ecology Progress Series*, **441**, 79-87.

Cigliano M, Gambi MC, Rodolfo-Metalpa R, Patti FP, Hall-Spencer JM (2010) Effects of ocean acidification on invertebrate settlement at volcanic CO_2 vents. *Marine Biology*, **157**, 2489-2502.

Connell SD, Russell BD (2010) The direct effects of increasing CO_2 and temperature on non-calcifying organisms: increasing the potential for phase shifts in kelp forests. *Proceedings of the Royal Society of London, B*, **277**, 1409-1415.

Dickson AG (2010) The carbonate system in seawater: equilibrium chemistry and measurements. In: *Guide to best practises for ocean acidification research and data reporting* (eds Riebesell, Fabry VJ, Hansson L, Gattuso J-P) Luxembourg: Publications Office of the European Union.

Dickson AG (1990) Standard potential of the ($AgCl + 1/2\ H_2 = Ag + HCl(aq)$) cell and the association of bisulfate ion in synthetic sea water from 273.15 to 318.15 K. *Journal of Chemical Thermodynamics*, **22**, 113-127.

572

573 Diaz-Pulido G, Gouezo M, Tilbrook B, Dove S, Anthony KRN (2011) High CO_2 enhances
574 the competitive strengths of seaweeds over coral. *Ecology Letters*, **14**, 156-162.
575

576 Doney SC, Fabry VJ, Feely RA, Kleypas JA (2009) Ocean Acidification: The other CO_2
577 problem. *Annual Review of Marine Science*, **1**, 169-92.
578

579 Doropoulous C, Ward S, Diaz-Pulido G, Hoegh-Guldberg O, Mumby PJ (2012) Ocean
580 acidification reduces coral recruitment by disrupting intimate larval-algal settlement
581 interactions. *Ecology Letters,* doi: 10.1111/j.1461-0248.2012.01743
582

583 Dupont S, Ortega-Martinez O, Thorndyke M (2010) Impact of near-future ocean acidification
584 on echinoderms. *Ecotoxicology,* **19**, 3, 449-462.
585

586 Einav R, Breckle S, Beer S (1995) Ecophysiological adaptation strategies of some intertidal
587 marine macroalgae of the Israeli Mediterranean coast. *Marine Ecology Progress Series*, **125**,
588 219-228.
589

590 Fabricius KE, Langdon C, Uthicke S, *et al*. (2011) Losers and winners in coral reefs
591 acclimatized to elevated carbon dioxide concentrations. *Nature Climate Change*, **1**, 165-169.
592

593 Gao K, Aruga Y, Asada K, Kiyohara M (1993a) Influence of enhanced CO_2 on growth and
594 photosynthesis of the red algae *Gracilaria* sp. and *G. chilensis*. *Journal of Applied*
595 *Phycology*, **5**, 563–571.
596

Gao K, Aruga Y, Asada K, Ishihara T, Akano T, Kiyohara M (1993b) Calcification in the articulated coralline alga *Corallina pilulifera*, with special reference to the effect of elevated CO_2 concentration. *Marine Biology*, **117**, 129–132.

Gao K, Zheng Y (2010) Combined effects of ocean acidification and solar UV radiation on photosynthesis, growth, pigmentation and calcification of the coralline alga *Corallina sessilis* (Rhodophyta). *Global Change Biology*, **16**, 2388–2398.

Gattuso JP, Allemand D, Frankignoulle M (1999) Photosynthesis and calcification at cellular, organismal and community levels in coral reefs: A review on interactions and control by carbonate chemistry. *American Zoologist*, **39**, 160–183.

Genty B, Briantais JM, Baker NR (1989) The relationship between the quantum yield of photosynthetic electron-transport and quenching of chlorophyll fluorescence. *Biochimica Et Biophysica Acta*, **990**, 87-92.

Häder DP, Lebert M, Mercado J, Aguilera J, Salles S, Flores-Moya A, Jiménez C, Figueroa, FL (1996) Photosynthetic oxygen production and PAM fluorescence in the brown alga *Padina pavonica* (Linnaeus) Lamouroux measured in the field under solar radiation. *Marine Biology*, **127**, 61-66.

Hall-Spencer JM, Rodolfo-Metalpa R, Martin S, Ransome E, Dine M, Turner SM, Rowley SJ, Tedesco D, Buia MC (2008) Volcanic carbon dioxide vents show ecosystem effects of ocean acidification. *Nature*, **454**, 96-99.

622 Harries DB, Harrow S, Wilson JR, Mair JM, Donnan DW (2007) The establishment of the
623 invasive alga *Sargassum muticum* on the west coast of Scotland: a preliminary assessment of
624 community effects. *Journal of the Marine Biological Association of the UK*, **87**, 1057-1067.
625
626 Hepburn CD, Pritchard DW, Cornwall CE, McLeod RJ, Beardall J, Raven JA, Hurd CL
627 (2011) Diversity of carbon use strategies in a kelp forest community: implications for a high
628 CO_2 Ocean. *Global Change Biology*, **17**, 2488-2497.
629
630 Hereu B (2006) Depletion of palatable algae by sea urchins and fishes in a Mediterranean
631 subtidal community. *Marine Ecology Progress Series*, **313**, 95–103.
632
633 Hernández JC, Clement S, Sangil C, Brito A (2008) The key role of the sea urchin *Diadema*
634 aff. *antillarum* in controlling macroalgae assemblages throughout the Canary Islands (eastern
635 subtropical Atlantic): An spatio-temporal approach. *Marine Environmental Research,* **66**,
636 259-270.
637
638 Hillis-Colinvaux, L (1980) Ecology and taxonomy of *Halimeda*: Primary producer of coral
639 reefs. *Advances in Marine Biology*, **17**, 1–327.
640
641 Hoffmann GE, Smith JE, Johnson KS *et al*. (2011) High-frequent dynamics of ocean pH: A
642 multi-ecosystem comparison. *PLoS One* **6**: doi:10.1371/journal.pone.0028983
643
644 Hoppe CJM, Langer G, Rokitta SD, Wolf-Gladrow DA, Rost B (2010) On CO_2 perturbation
645 experiments: over-determination of carbonate chemistry reveals inconsistencies.
646 *Biogeosciences Discussions,* **7**, 1707-1726.

Johnson VR, Brownlee, C, Rickaby REM, Graziano M, Milazzo M & Hall-Spencer, JM (2011) Responses of marine benthic microalgae to elevated CO_2. *Marine Biology* doi: 10.1007/s00227-011-1840-2.

IPCC (Intergovernmental Panel on Climate Change) (2007) Working Group 1 Report, The Physical Science Basis. http://ipcc-wg1.ucar.edu/wg1/wg1-report.html.

Kübler JE, Johnston AM, Raven JA (1999) The effects of reduced and elevated CO_2 and O_2 on the seaweed *Lomentaria articulata*. *Plant, Cell and the Environment*, **22**, 1303–1310.

Kuffner IB, Andersson AJ, Jokiel PL, Rodgers KS, Mackenzie FT (2008) Decreased abundance of crustose coralline algae due to ocean acidification. *Nature Geoscience*, **1**, 114-117.

Leinaas HP, Christie H (1996) Effects of removing sea urchins (*Strongylocentrotus droebachiensis*): stability of the barren state and succession of kelp forest recovery in the east Atlantic. *Oecologia*, **105**, 524–536

Lewis SM, Norris JN, Searles RB (1987) The regulation of morphological plasticity in tropical reef algae by herbivory. *Ecology*, **68**, 636-641.

Lewis E, Wallace WR (1998) Program developed for CO_2 system calculations. Carbon dioxide information analysis center, Oak Ridge National Laboratory, U.S. Department of Energy, Oak Ridge, TN.

672

673 Ling SD, Ibbott S, Sanderson JC (2010) Recovery of canopy-forming macroalgae following
674 removal of the enigmatic grazing sea urchin *Heliocidaris erythrogramma*. *Journal of*
675 *Experimental Marine Biology and Ecology*, **395**, 135-146.

676

677 Littler MM, Littler DS (1980) The evolution of thallus form and survival strategies in
678 benthic marine macroalgae: field and laboratory tests of a functional form model. *American*
679 *Naturalist*, **116**, 25-44.

680

681 Martin S, Gattuso J-P (2009) Response of Mediterranean coralline algae to ocean
682 acidification and elevated temperature. *Global Change Biology*, **15**, 2089-2100.

683

684 Martin S, Rodolfo-Metalpa R, Ransome E, Rowley S, Buia M-C, Gattuso J-P, Hall-Spencer
685 JM (2008) Effects of naturally acidified seawater on seagrass calcareous epibionts. *Biology*
686 *Letters*, **4**, 689-692.

687

688 Martone PT (2010) Quantifying growth and calcium carbonate deposition of *Calliarthron*
689 *cheilosporiodes* (Corallinales, Rhodophyta) in the field using a persistent vital stain. *Journal*
690 *of Phycology*, **46**, 13-17.

691

692 McClanahan TR (1994) Kenyan coral reef lagoon fish: effects of fishing, substrate
693 complexity, and sea urchins. *Coral Reefs*, **13**, 231–241.

694

695 McConnaghey T (1998) Acid secretion, calcification, and photosynthetic carbon
696 concentrating mechanisms. *Canadian Journal of Botany*, **76**, 1119–1126.

McConnaughey AT, Whelan JF (1997) Calcification generates protons for nutrient and bicarbonate uptake. *Earth Science Reviews*, **42**, 95–117.

McManus JW, Polsenberg JF (2004) Coral–algal phase shifts on coral reefs: Ecological and environmental aspects. *Progress in Oceanography*, 60, 263-279.

Miles H, Widdicombe S, Spicer JI, Hall-Spencer JM (2007) Effects of anthropogenic seawater acidification on acid base balance in the sea urchin *Psammechinus miliaris*. *Marine Pollution Bulletin*, **54**, 89–9.

Milliman JD (1974) Marine Carbonates, pp. 1-375, Springer, Berlin.

Mumby PJ, Hedley JD, Zychaluk K, Harborne AR, Blackwell PG (2006) Revisiting the catastrophic die-off of the urchin *Diadema antillarum* on Caribbean coral reefs: Fresh insights on resilience from a simulation model. *Ecological Modelling*, **196**, 131-148.

Nelson WA (2009) Calcified macroalgae-critical to coastal ecosystems and vulnerable to change: a review. *Marine and Freshwater Research*, **60**, 787-801.

Okazaki M, Pentecost A, Tanaka Y, Miyata M (1986) A study of calcium carbonate deposition in the genus *Padina* (Phaeophyceae, Dictyotales). *British Phycological Journal*, **21**, 217-24.

Orr JC, Fabry VJ, Aumont O *et al*. (2005) Anthropogenic ocean acidification over the twenty-first century and its impact on calcifying organisms. *Nature*, **437**, 681-686.

723

724 Padilla DK (1993) Rip-stop in marine algae: minimising the consequences of herbivore
725 damage. *Evolutionary Ecology*, **7**, 634-644.

726

727 Porzio L, Buia MC, Hall-Spencer JM (2011) Effects of ocean acidification on macroalgal
728 communities. *Journal of Experimental Marine Biology and Ecology*, **400**, 278-287.

729

730 Price NN, Hamilton SL, Tottell JS, Smith JE (2011) Species-specific consequence of ocean
731 acidification for the calcareous tropical green algae *Halimeda*. *Marine Ecology Progress*
732 *Series*, **440**, 67-78.

733

734 Ralph PJ, Gademan R (2005) Rapid light curves: a powerful tool to assess photosynthetic
735 activity. *Aquatic Botany*, **82**, 222-237.

736

737 Raven, JA (2011) Effects on marine algae of changed seawater chemistry with increasing
738 Atmospheric CO_2. *Biology and Environment: Proceedings of the Royal Irish Academy*, **111**B,
739 1–17.

740

741 Reiskind JB, Seamon PT, Bowes G (1988) Alternative methods of photosynthetic carbon
742 assimilation in marine macroalgae. *Plant Physiology*, **87**, 686–692.

743

744 Riebesell U (2008) Acid test for marine biodiversity. *Nature*, **454**, 46-47.

745

746 Ritchie R (2006) Consistent sets of spectrophotometric chlorophyll equations for
747 acetone, methanol and ethanol solvents. *Photosynthesis Research*, **89**, 27-41.

748

749 Robbins LL, Knorr PO, Hallock P (2009) Response of *Halimeda* to ocean acidification: field
750 and laboratory evidence. *Biogeosciences Discussions*, **6**, 4895-4918.

751

752 Rodolfo-Metalpa R, HoulbrèqueF, Tambutté É, Boisson F, Baggini C, Patti FP, Jeffree R,
753 Fine M, Foggo A, Gattuso JP, Hall-Spencer JM (2011) Coral and mollusc resistance to ocean
754 acidification adversely affected by warming. *Nature Climate Change*, **1**, 308-312.

755

756 Roleda MY, Morris JN, McGraw CM, Hurd CL (2011) Ocean acidification and seaweed
757 reproduction: increased CO2 ameliorates the negative effect of lowered pH on meiospore
758 germination in the giant kelp *Macrocystis pyrifera* (Laminariales, Phaeophyceae). *Global*
759 *Change Biology* doi:10.1111/j.1365-2486.2011.02594.x.

760

761 Roy RN, Vogel KM, Porter-Moore C, Pearson T, Good CE, Millero FJ, Campbell DM
762 (1993) The dissolution of constants of carbonic acid in seawater at salinities 5 to 45 and
763 temperatures 0 to 45 °C. *Marine Chemistry*, **4**, 249-267.

764

765 Russell BD, Thompson J-A I, Falkenberg LJ, Connell SD (2009) Synergistic effects of
766 climate change and local stressors: CO_2 and nutrient-driven change in subtidal rocky habitats.
767 *Global Change Biology*, **15**, 2153-2162.

768

769 Russell BD, Harley CDG, Wernberg T, Mieszkowska N, Widdicombe S, Hall-Spencer JM
770 (2011a) Predicting ecosystem shifts requires new approaches that integrate the effects of
771 climate change across entire systems. *Biology Letters*, doi: 10.1098/rsbl.2011.0779

772

773 Russell BD, Passarelli CA, Connell SD (2011b) Forecasted CO_2 modifies the influence of
774 light in shaping subtidal habitat. *Journal of Phycology*, **47,** 744-752.
775
776 Sala E, Boudouresque CF, Harmelin-Vivien ML (1998) Fishing, trophic cascades, and the
777 structure of algal assemblages: evaluation of an old but untested paradigm. *Oikos*, **82**, 425-
778 439.
779
780 Sammarco PW, Levington JS, Ogden JC (1974) Grazing and control of coral reef community
781 structure by *Diadema antillarum* Philippi (Echinodermata:Echinoidea): a preliminary study.
782 *Journal of Marine Research*, **32**, 47-53.
783
784 Sammarco PW (1982). Effects of grazing by *Diadema antillarum* Philippi (Echinodermata:
785 Echinoidea) on algal diversity and community structure. *Journal of Experimental Marine*
786 *Biology and Ecology*, **65**, 83-105.
787
788 Semesi IS, Kangwe J, Björk M (2009) Alterations in seawater pH and CO_2 affect
789 calcification and photosynthesis in the tropical coralline alga, *Hydrolithon* sp. (Rhodophyta).
790 *Estuarine and Coastal Shelf Science*, **84**, 337-341.
791
792 Sinutok S, Hill R, Doblin MA, Wuhrer R, Ralph PJ (2011) Warmer more acidic conditions
793 cause decreased productivity and calcification in subtropical coral reef sediment-dwelling
794 calcifiers. *Limnology and Oceanography*, **56**, 1200-1212.
795

Villouta E, Chadderton, WL, Pugsley, CW, Hay CH (2001) Effect of sea urchin (*Evechinus chloroticus*) grazing in Dusky Sound, Fiordland, New Zealand. *New Zealand Journal of Marine and Freshwater Research*, **35**, 1007-1024.

Wefer G (1980) Carbonate production by algae *Halimeda*, *Penicillus* and *Padina*. *Nature*, **285**, 323-324.

Wernberg T, Smale DA, Thomson MS (2012) A decade of climate change experiments on marine organisms: procedures, patterns and problems. *Global Change Biology* (in press).

Widdicombe S, Spicer JI (2008) Predicting the impact of ocean acidification on benthic biodiversity: What can physiology tell us? *Journal of Experimental Marine Biology and Ecology*, **366**, 187-197.

Table 1. Seawater carbonate chemistry measurements for each study station off the island of Vulcano (V) and in Papua New Guinea; Upa-Upasina (U) and Esa'Ala (E), R= reference station, S = elevated CO_2 station. In Vulcano, temperature (range 18.6-27.7 °C), pH and salinity (= 38) were measured in Sept-Oct 2009, April 2010, July 2010, Sept-Oct 2010, May 2011, Sept-Oct 2011. In Papua New Guinea temperature (range 28.2-31.4 °C), pH and salinity (= 34) were measured in April 2011. The pH and total alkalinity (Vulcano: mean TA, *n* = 3; PNG: median TA values taken from Fabricius *et al*., 2011) were used to calculate the remaining parameters using CO2 SYS programme (using the constants of Roy *et al.* 1993 and Dickson 1990 for KSO_4).

Site & Station		pH range (NBS scale)	*p*CO2 (µatm)	TA (mmol kg^{-1})	DIC (mmol kg^{-1})	CO_3^{2-} (mmol kg^{-1})	HCO_3^- (mmol kg^{-1})	$\Omega_{calcite}$	$\Omega_{aragonite}$
	max	8.35	241	2.682	2.402	0.18	2.206	4.27	2.69
V R1	median	8.17	388	(±0.12)	2.492	0.13	2.341	2.99	1.89
	min	8.06	513		2.538	0.10	2.405	2.39	1.51
	max	8.29	274	2.591	2.349	0.16	2.177	3.67	2.31
V R2	median	8.18	365	(±0.03)	2.399	0.12	2.251	2.95	1.86
	min	8.08	471		2.442	0.10	2.311	2.40	1.51
	max	8.29	272	2.579	2.337	0.15	2.165	3.65	2.30
V R3	median	8.18	364	(±0.04)	2.394	0.12	2.247	2.94	1.85
	min	8.10	446		2.421	0.11	2.288	2.49	1.57
	max	8.22	355	2.790	2.569	0.15	2.401	3.44	2.17
V S1	median	8.08	510	(±0.08)	2.641	0.11	2.499	2.60	1.64
	min	7.76	1119		2.752	0.06	2.627	1.31	0.82
	max	8.10	474	2.742	2.578	0.11	2.436	2.65	1.67
V S2	median	7.71	1244	(±0.07)	2.727	0.05	2.601	1.15	0.73
	min	7.07	5628		3.054	0.01	2.697	0.27	0.17
	max	8.24	337	2.796	2.565	0.15	2.392	3.59	2.27
V S3	median	7.66	1428	(±0.12)	3.794	0.04	2.662	1.05	0.66
	min	6.80	10,730		3.428	0.01	2.762	0.15	0.09
	max	8.32	268	2.296	1.869	0.31	1.556	7.47	4.97
U R1	median	8.31	276		1.875	0.30	1.566	7.38	4.90
	min	8.29	292		1.887	0.29	1.585	7.18	4.78

	max	8.23	351	2.296	1.930	0.27	1.655	6.49	4.31
U R2	median	8.22	361		1.935	0.26	1.664	6.40	4.25
	min	8.21	372		1.943	0.26	1.676	6.27	4.17
	max	8.87	1130	2319	2.174	0.13	2.019	3.06	2.04
U S1	median	7.78	1218		2.189	0.12	2.041	2.84	1.89
	min	7.76	1283		2.197	0.11	2.052	2.72	1.81
	max	7.58	2029	2319	2.263	0.08	2.132	1.92	1.28
U S2	median	7.47	2665		2.031	0.06	2.170	1.53	1.02
	min	7.46	2724		2.306	0.06	2.175	1.47	0.98
	max	8.27	309	2288	1.872	0.30	1.564	7.36	4.93
E R1	median	8.2	380		1.915	0.27	1.635	6.66	4.47
	min	8.03	620		2.026	0.20	1.813	4.85	3.25
	max	8.00	677	2298	2.050	0.19	1.843	4.65	3.12
E S1	median	7.89	914		2.104	0.16	1.926	3.82	2.56
	min	7.74	1338		2.184	0.11	2.043	2.60	1.73
	max	7.29	4063	2298	2.348	0.04	2.201	0.99	0.66
E S2	median	6.56	23,095		2.853	0.09	2.278	0.21	0.14
	min	6.43	21,204		3.057	0.06	2.283	0.16	0.10

832

833

834

835

836

837

838

839

840

841

842

Table 2. Changes in (a) *Padina* spp. cover, (b) urchin abundances and (c) $CaCO_3$ content of *Padina* spp. fronds, along the three pH gradients at Esa'Ala, Upa-Upasina and Vulcano. Generalised linear model outputs. Data in bold indicate significant effect of pH ($P<0.05$).

a)	**Estimate**	**SE**	**t**	***P***
Region.Esa	14.03	4.31	3.26	0.008
Region.Upa	22.83	8.74	2.61	0.024
Region.Vul	17.05	7.32	2.33	0.040
RegionEsa : pH	-1.38	0.57	-2.43	**0.033**
RegionUpa : pH	-4.28	0.96	-4.48	**0.001**
RegionVul : pH	-3.48	0.74	-4.70	**0.001**
b)	**Estimate**	**SE**	**t**	***P***
Region.Esa	-27.82	8.56	-3.25	0.006
Region.Upa	-0.31	0.51	-0.61	0.553
Region.Vul	-0.66	0.46	-1.43	0.176
pH	3.40	1.06	3.22	**0.007**
c)	**Estimate**	**SE**	**t**	***P***
Region. Esa	-5.07	2.19	-2.32	0.082
RegionUpa	-7.38	7.03	-1.05	0.353
RegionVul	-21.20	4.83	-4.39	0.012
RegionEsa : pH	0.70	0.29	2.38	0.076
RegionUpa : pH	1.52	0.83	1.84	0.140
RegionVul : pH	3.25	0.54	6.06	**0.004**

Table 3. Mean (± SE) abundance, length and width of aragonite crystals deposited by *Padina pavonica* along the Vulcano CO_2 gradient. Data derived from SEM analysis of fronds (n = 3 fronds per station), over calcified apical regions only (see frond images in Fig. 5), therefore do not reflect total means for whole fronds.

Station	Mean no. crystals (per 5 µm^2)	Mean crystal length (µm)	Mean crystal width (µm)
V-R1	94 ± 6.65	1.30 ± 0.05	0.20 ± 0.01
V-R2	96 ± 7.47	1.44 ± 0.07	0.20 ± 0.01
V-R3	96 ± 8.20	1.43 ± 0.06	0.21 ± 0.01
V-S1	106 ± 4.76	1.80 ± 0.06	0.18 ± 0.01
V-S2	115 ± 8.74	1.54 ± 0.10	0.19 ± 0.01
V-S3	153 ± 6.31	1.52 ± 0.07	0.17 ± 0.01

867

868 **Figure Legends**

869

870 **Fig. 1** Range in pH_{NBS} (<0.5 m water depth) across CO_2 gradients in a) Vulcano (Sicily; *n* =
871 22-27 per station) **b)** Upa-Upasina (Papua New Guinea; *n* = 6 per station) **c)** Esa'Ala (Papua
872 New Guinea; *n* = 7 & S2, *n* = 9). 'R' denotes reference stations, 'S' denotes elevated CO_2
873 stations.

874

875 **Fig. 2** Images showing an urchin and coralline algae dominated rocky shore under ambient
876 CO_2 **(a)** in Ischia, Italy (photograph by David Liittschwager, National Geographic) and the
877 proliferation of Phaeophyta at elevated CO_2 at vent sites in Ischia (photograph by Luca
878 Tiberti, Associazione Nemo) **(b)**. *Padina australis* showing normal calcification at tropical
879 (Papua New Guinea) reference station, Esa'Ala R1 **(c**; scale bar = 1 cm**)** and visibly low
880 calcification at Esa'Ala S1 **(d)**. Arrows indicate CO_2 vent bubbles.

881

882 **Fig. 3**

883 Mean percentage cover (histogram + SE) of *Padina* spp. and abundance of sea urchins (mean
884 ± SE) along CO_2 gradients at **a)** Vulcano **b)** Upa-Upasina **c)** Esa'Ala (*n* = 20 quadrats per
885 station). Mean pH (*n* = 6-27 per station) of each station indicated.

886

887 **Fig. 4**

888 **a)** Mean (+ SE) $CaCO_3$ content of *Padina* spp. along CO_2 gradients at **a)** Vulcano (*n* = 30 per
889 station), **b)** Upa-Upasina (*n* = 15 per station) and **c)** Esa'Ala) (*n* = 5 per station).

890

Fig. 5 Mean (+ SE) chl *a* content in *P. pavonica* fronds along the Vulcano CO_2 gradient (n = 40 per station). Images illustrate changes in $CaCO_3$ deposition on *P. pavonica* frond surfaces at V-R2 and V-S2 along the Vulcano CO_2 gradient. All thalli at V-R1- V-R3 were heavily calcified, all thalli at S1-S3 were more lightly calcified, calcification appears to be limited to thin bands along apical regions (scale bar = 1 cm). Arrows indicate locations of SEM analyses.

Fig. 6 Rapid light curves of *P. pavonica* along the Vulcano CO_2 gradient, showing the mean (± SE) relative electron transport rates (*r*ETR) per station (n = 5 for V-R3 + V-S3, n = 6 for all other stations) at increasing irradiance.

903 **Figure 1**

904

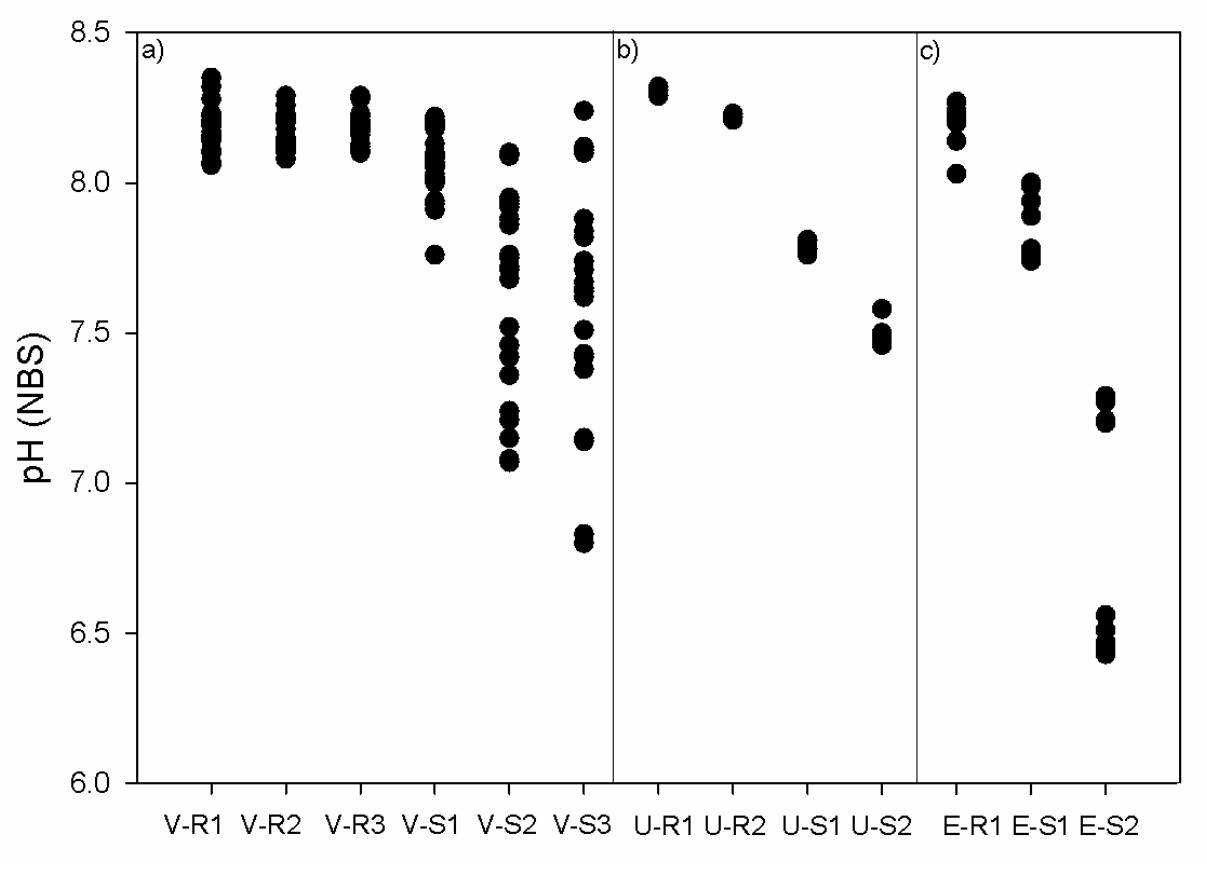

905

906

907 **Figure 2.**

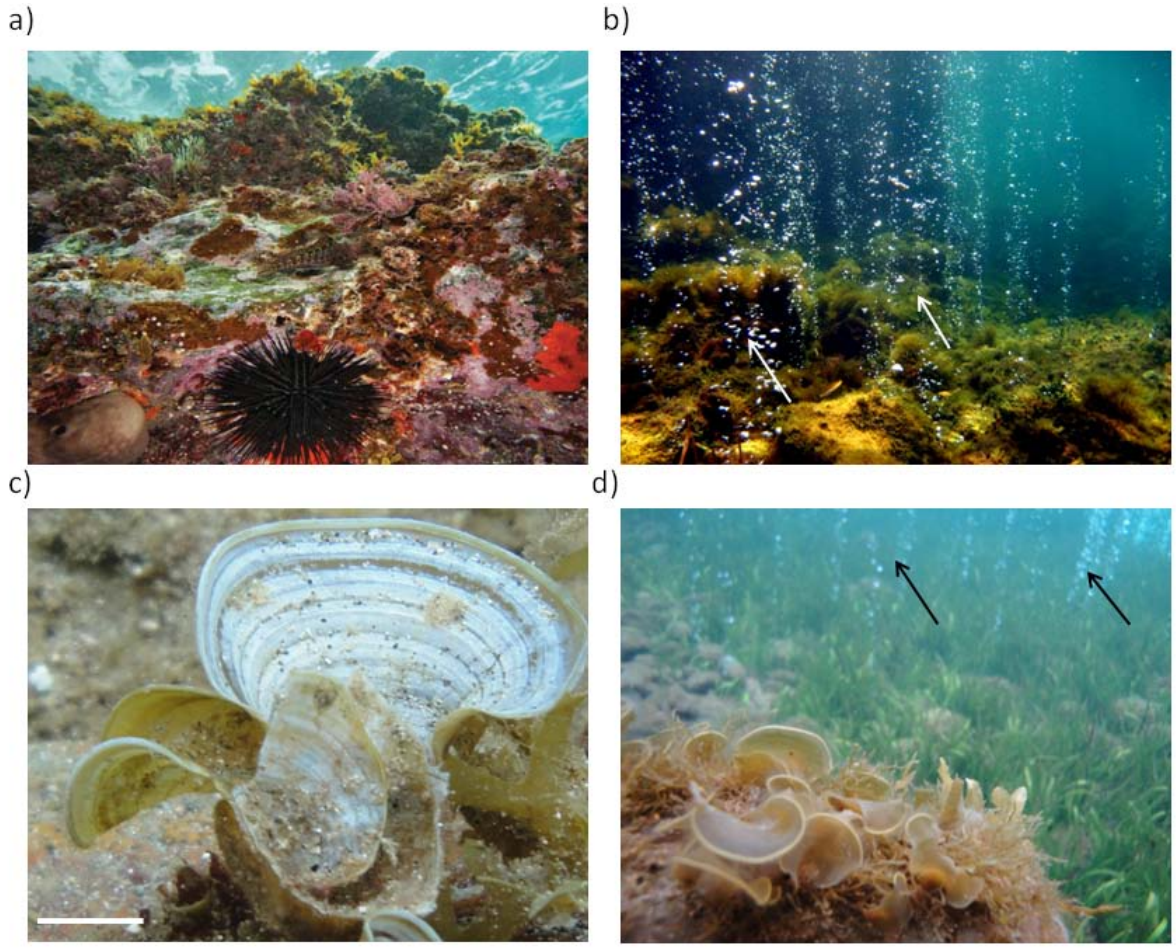

908

909

Figure 3.

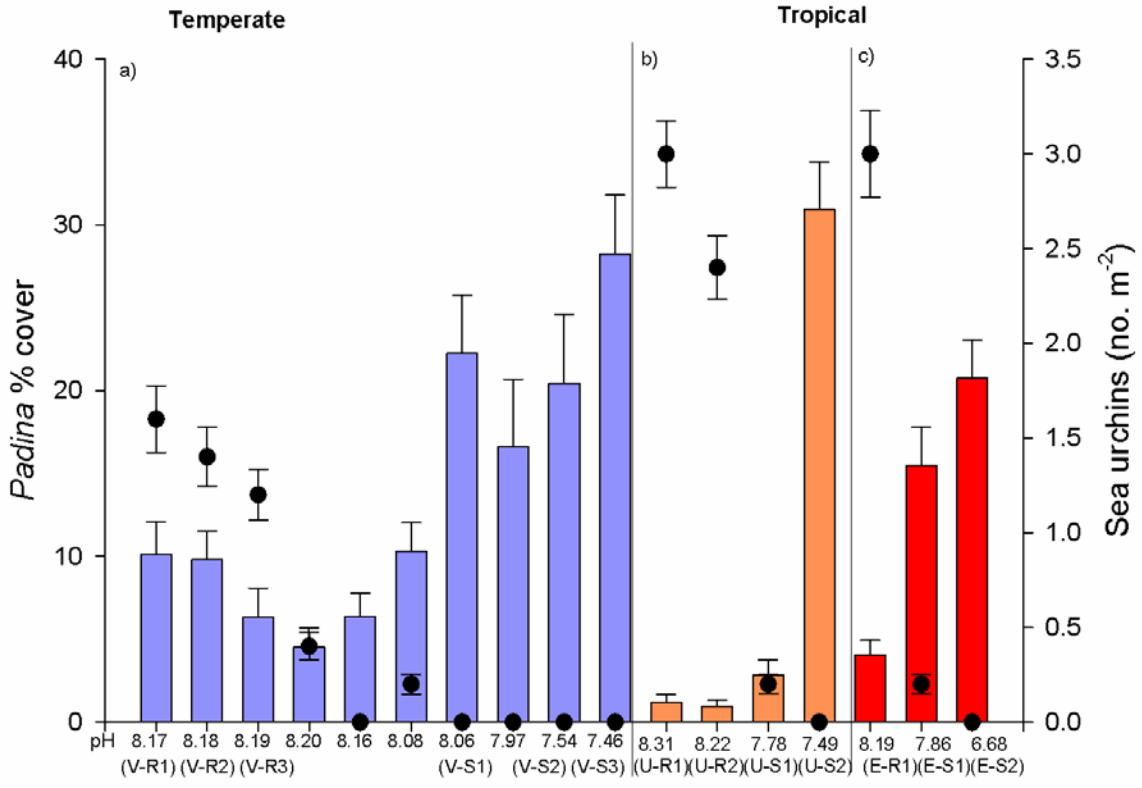
Temperate
Tropical
a)
b)
c)
Padina % cover
Sea urchins (no. m-2)
40
30
20
10
0
3.5
3.0
2.5
2.0
1.5
1.0
0.5
0.0
pH 8.17 8.18 8.19 8.20 8.16 8.08 8.06 7.97 7.54 7.46 8.31 8.22 7.78 7.49 8.19 7.86 6.68
(V-R1) (V-R2) (V-R3) (V-S1) (V-S2) (V-S3) (U-R1) (U-R2) (U-S1) (U-S2) (E-R1) (E-S1) (E-S2)

913 **Figure 4.**

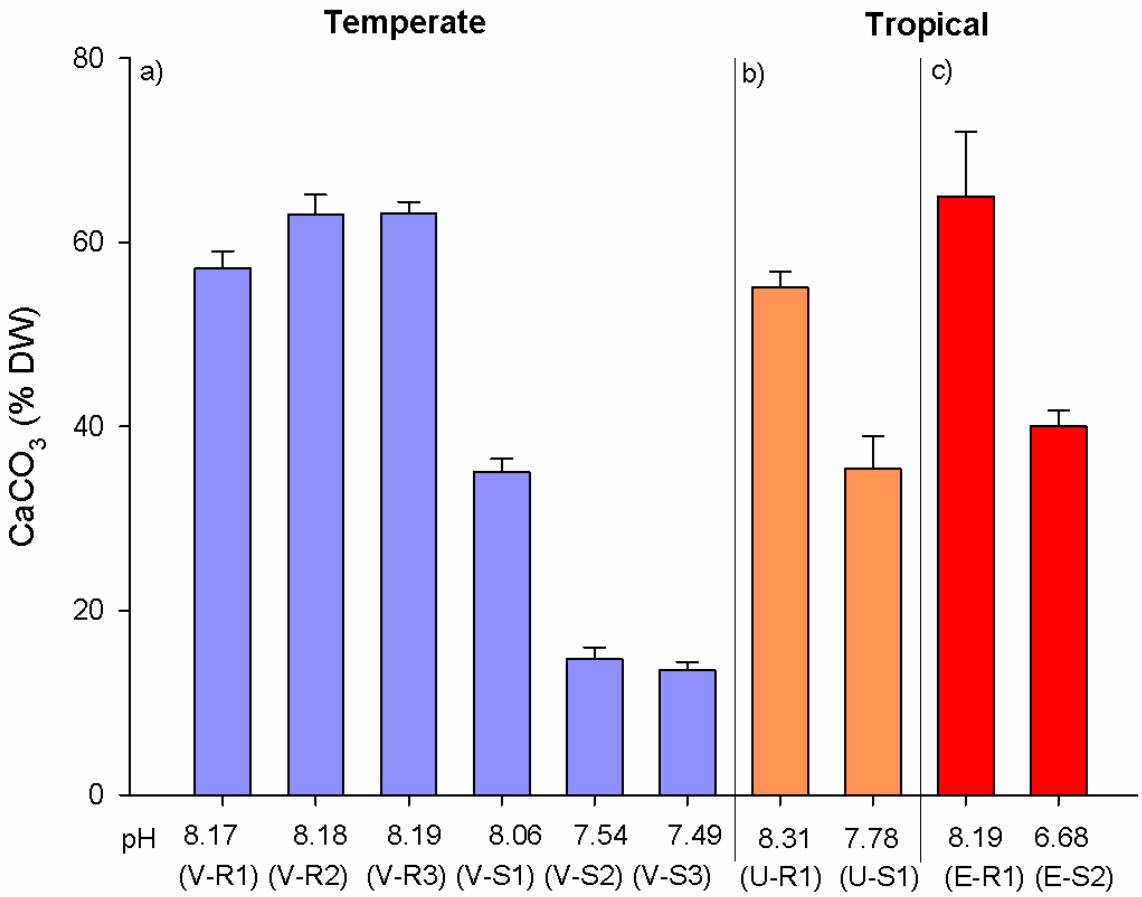

914

915

916 **Figure 5.**

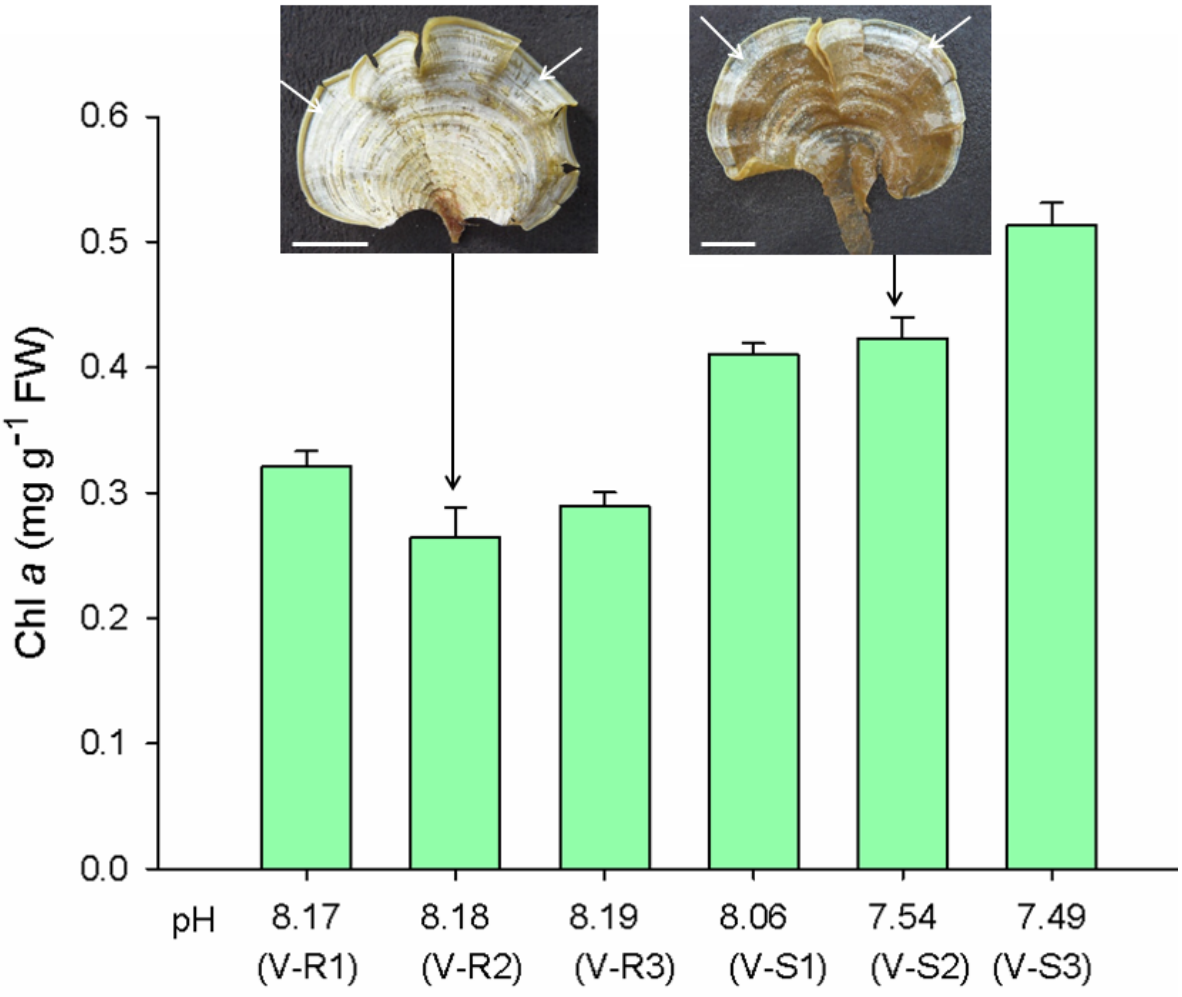

917

918

919 **Figure 6.**

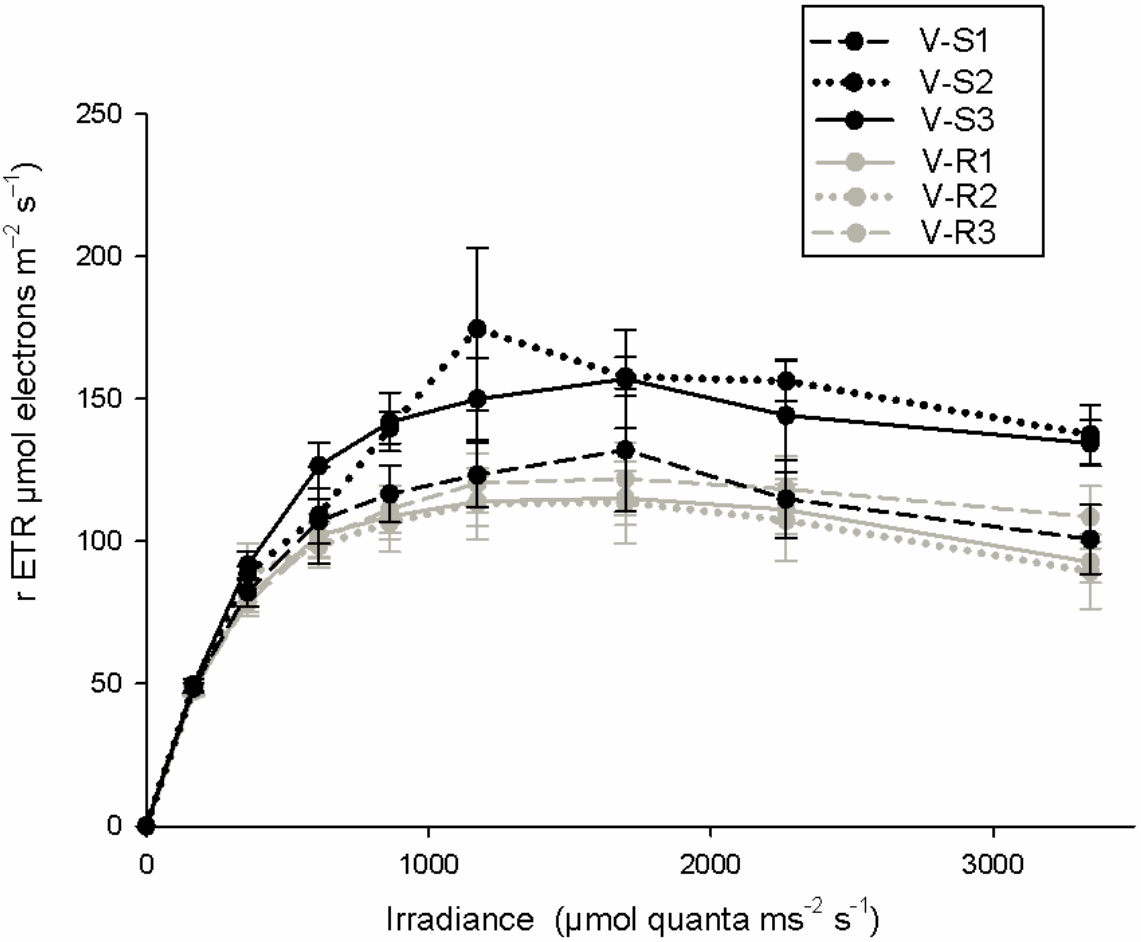

920

921